Chemical relaxation time of pions in hot hadronic matter

Chungsik Song and Volker Koch
Nuclear Science Division, MS70A-3307, Lawrence Berkeley National Laboratory, Berkeley, California 94720
(Received 18 November 1996)

We calculate characteristic time scales for the chemical equilibration of pions in hot hadronic matter using an effective chiral Lagrangian. We find that inelastic processes involving vector and axial vector mesons reduce the chemical equilibration time by a factor of ~ 10 compared to the result previously calculated in chiral perturbation theory. For a temperature of $T \sim 160$ MeV we obtain a chemical relaxation time of $\tau_{\rm ch} \simeq 7$ fm/c, which is comparable with typical time scales for a hadronic system generated in SPS-energy heavy-ion collisions. The effect of baryons is also estimated and found to be negligible for SPS energies but might be important for AGS energies. We predict that chemical freeze-out should take place at considerably higher temperatures $\Delta T \simeq 40$ MeV than thermal freeze-out and that the hadronic phase would not sustain a pion chemical potential larger than 50 MeV. [S0556-2813(97)04406-3]

PACS number(s): 25.75.−q, 12.39.Fe, 14.40.Aq, 12.38.Mh

I. INTRODUCTION

High-energy nucleus-nucleus collisions offer a unique opportunity to explore the large-scale properties of quantum chromodynamics, in particular its phase structure at high temperatures and densities [1]. For sufficiently high collision energy, we expect a phase transition into a locally thermalized, deconfined plasma of quarks and gluons, the so-called quark-gluon plasma (QGP) [2]. There may be two different phase transitions, deconfinement and chiral phase transition, in QCD at high temperature and/or density. The nature and order of the phase transition have been studied as well as possible signatures for the new phase of hadronic matter.

Certainly the system produced in these collisions is not immediately in thermal and chemical equilibrium. Secondary interactions among the produced particles are necessary to achieve equilibrium. If equilibrium is reached, global observables such as transverse energy production can be related to thermodynamic variables, such as energy and entropy density, commonly used to characterize these collisions. One can also use the hydrodynamic equations to study the evolution of the hadronic system at finite temperature and/or density. These conditions considerably facilitate the calculation of certain quark-gluon plasma signals, such as the yields of photons, lepton pairs, strangeness, and hadrons containing heavy quarks. However, even if the heavy-ion collision is energetic enough to fully equilibrate the system at early time, e.g., in the quark-gluon plasma phase, the system will not necessarily remain equilibrated as it expands. Only when the collision rate is greater than the expansion rate will equilibrium be maintained. It is therefore crucial to understand the following questions: How does the system approach equilibrium? What are the time scales for thermal and chemical equilibration, and to which extent is equilibrium maintained in the hadronic phase before the system breaks up into the final state hadrons?

Recently the question of thermodynamic equilibration in the early stages of collisions at RHIC and LHC has been studied in the parton model [3–5]. In the partonic system created early in the collisions, gluons are the dominant components of the system. They reach thermal equilibrium on the time scale 0.3–0.5 fm/c after collision with an undersaturated gluon density. The thermalization of quarks follows that of gluons with the time scale 1 fm/c and reaches chemical equilibrium later since the quark pair production by gluon fusion and the decay of gluons occur at a somewhat smaller rate. These thermodynamic equilibration conditions would be observed in open charm, photon, dilepton, and J/ψ production.

The question of equilibration in the hadronic phase, on the other hand, has been addressed by analyzing the observed hadron abundances and spectral distributions [6–11]. The prevailing view requires first a chemical freeze-out, from which particle abundances are preserved, followed by a thermal freeze-out, after which all interactions between the produced particles have ceased. Since the system remains in local thermal equilibrium, the state can be characterized by a maximum of the entropy consistent with the conservation laws for energy and momentum and of the relevant particle number. Neglecting dissipative processes, the corresponding continuity equations then imply that entropy is conserved; i.e., the expansion is an adiabatic process. If so, the hadronic system is described by two parameters, temperature $T(x)$ and a ''chemical potential''[1] $\mu_i(x)$ for each species. Assuming such a partial equilibrium, i.e., thermal but not chemical, the observed hadronic abundance can be well described.

As far as strange degrees of freedom are concerned, one expects only a partial saturation since the time scale for strangeness saturation is normally larger than the collision time scale. The chemical properties of strange particles at freeze-out are regarded as an important ingredient to understand strangeness production in high-energy nucleus-nucleus collisions [12].

Naturally, hadronic observables can only tell us something about the conditions at freeze-out. In this paper, we are interested in the thermal and chemical equilibrium conditions

[1]A detailed discussion of the meaning of the ''chemical potential'' will be given at the beginning of Sec. II B.

 © 1997 The American Physical Society

of pions in hot hadronic matter at temperatures higher than the freeze-out temperature in order to see if the observed freeze-out conditions can be understood within a pure hadronic model. We use an effective chiral Lagrangian with vector and axial vector mesons to describe the interaction of pions in hadronic matter. In Sec. II, we first consider the processes that lead to thermal equilibrium for pions in hot hadronic matter. Elastic pion collisions $\pi+\pi\rightarrow\pi+\pi$ turn out to be the principal thermalizing process. Second, we clarify the meaning of chemical equilibrium and chemical potential of pions in hot matter produced in high-energy nucleus-nucleus collisions. Third, we estimate the characteristic time scale for chemical equilibrium of pions in hadronic matter, first with pions, and then later including resonances. Finally, we also explore the effect of baryons on the chemical equilibrium conditions of pions in hot hadronic matter. In Sec. III, the time scales for the chemical equilibrium of pions are studied, assuming a finite pion chemical potential.

II. THERMODYNAMIC EQUILIBRATION OF PIONS

The thermodynamic equilibration in a hadronic system is driven by multiple collisions among particles in the system. Generally the equilibration time is directly proportional to the collision rate. In an expanding system, therefore, the collision rate should be much larger than the expansion rate of the system in order to maintain thermodynamic equilibrium. As long as the expansion velocity of the system does not exceed the most probable velocity of the thermal particles in the system, this condition is satisfied if the mean free path of a particle is shorter than the size of the system. In the following we determine the thermal and chemical relaxation time of pions, assuming that the system is slightly deviated from the equilibrium state, i.e., in the relaxation time approximation.

A. Thermal equilibrium

At low temperatures hadronic matter, which mainly consists of pions, can be analyzed systematically in the framework of chiral perturbation theory at finite temperature. The low-energy theorems, which are obtained from current algebra and partial conservation of axial vector current (PCAC), can be translated into a corresponding set of exact statements concerning the coefficients of the low-temperature expansion. Since typical pion energies are of the order $E\sim T$ at finite T, interactions among pions generate power corrections, controlled by the expansion parameter T^2/f_π^2, where $f_\pi=93$ MeV is the pion decay constant [13]. It is therefore possible to treat the interaction in low-temperature pion gas as a perturbation.

The thermal equilibration of pions at low temperatures will be governed by elastic two-body collisions, $\pi+\pi\rightarrow\pi+\pi$, since inelastic processes contribute in the next leading order in the low-energy expansion. As long as we consider elastic two-body collisions, the thermal relaxation time $\tau_{\rm th}$ is given by [14]

$$\frac{1}{\tau_{\rm th}}=\frac{1}{2}(1-e^{-\beta E_a})\frac{1}{2E_a}\int\frac{d^3p_2}{(2\pi)^3 2E_2}\frac{d^3p_3}{(2\pi)^3 2E_3}\times\frac{d^3p_4}{(2\pi)^3 2E_4}(2\pi)^4\delta^4(p_a+p_2-p_3-p_4)\times\sum_{2,3,4}|\mathcal{M}(\pi_a\pi_2\rightarrow\pi_3\pi_4)|^2 f_2(1+f_3)(1+f_4), \tag{2.1}$$

where f_i's are Bose-Einstein distribution functions. The factor of 1/2 comes from the identity of particles at the final state and the sum is over the spin and isospin degeneracy of particles 2, 3, and 4. The second term ($\sim e^{-\beta E}$) indicates the contribution from the inverse reaction. Note that this result is obtained in the relaxation time approximation. In the classical limit where Bose-Einstein or Fermi-Dirac quantum statistics is approximated by Boltzmann statistics, this can be written as

$$\frac{1}{\tau_{\rm th}}=(1-e^{-\beta E_a})\int\frac{d^3p_2}{(2\pi)^3}\sum_2\ \sigma(a2\rightarrow 34)v_{a2}e^{-E_2/T}, \tag{2.2}$$

where σ is the cross section corresponding to the relevant reaction and v_{a2} is the relative velocity.

The mean relaxation time is defined as

$$\overline{\tau}_{\rm th}=\frac{1}{\int d^3p_a f_a(p_a)}\int d^3p_a\tau_{\rm th}(p_a)f_a(p_a). \tag{2.3}$$

To a good approximation, the result for the thermal relaxation time is given by [14]

$$\overline{\tau}_{\rm th}\approx\frac{12f_\pi^4}{T^5}. \tag{2.4}$$

At $T=150$ MeV the relaxation time turns out to be about 2 fm/c. Since the mean free path $\lambda\approx c\tau$ in the relativistic limit, the result can be compared to the size of the system. Here we assume that the radius of the hot matter would be 5–10 fm. This implies that pions are in thermal equilibrium in hadronic matter, mainly due to the two-body elastic collisions.

At temperatures close to the phase transition, other heavy mesons like kaons, vector mesons, etc., become increasingly abundant and reduce the thermalization time even further. Thus, we conclude that pions can maintain thermal equilibrium in hot hadronic matter even at comparatively low temperatures. From formula (2.4) we expect a freeze-out temperature $\leqslant 130$ MeV for a small system such as S+S or S+Au. This is somewhat lower than the values extracted from experiment, which are $\sim$ 150 MeV. The reason for this slight discrepancy is most likely due to the flow generated in the reaction, which reduces the effective system size.

We also expect that light vector mesons ρ, ω, and ϕ reach thermal equilibrium in hot hadronic matter. For ρ and ω the dominant reactions will be the collisions with thermal pions through heavy resonances such as $\pi+\rho\rightarrow a_1\rightarrow\pi+\rho$ and $\pi+\omega\rightarrow b_1\rightarrow\pi+\omega$; see Ref. [15]. In this reference it has

also been shown that the various collisions in hot hadronic matter make it possible for phi mesons to be in thermal equilibrium.

B. Chemical potential of pions in hot hadronic matter

Before we embark on the discussion of chemical equilibrium we should first clarify what we mean when we talk about a ''chemical potential'' in the subsequent paragraphs. Strictly speaking, a chemical potential is associated with a conserved quantity. In the case of pions, the conserved quantity would be the charge and, therefore, the only rigorously defined chemical potential would be associated with the charge of the pions (and all other particles involved in the system for that matter). This chemical potential, let us call it μ_{charge}, enters with opposite signs in the Bose-Einstein distribution functions for π^+ and π^-. In the following discussion we will always consider a charge-neutral system and, therefore, $\mu_{\text{charge}}=0$.

The pion number is not conserved because of possible particle and antiparticle production (or annihilation) due to the electromagnetic or weak processes. However, the lifetime of a system created in a relativistic heavy-ion collisions is too short in order for the electromagnetic and weak processes to be relevant, so that we can safely ignore them from now on. Let us also assume, for a moment, that the time scale for the strong number-changing processes are long compared to the lifetime of the system, whereas the elastic processes, which are responsible for kinetic equilibration, are fast. In this case, the number of pions does not change, and after kinetic equilibrium has been established, the pions are distributed according to a Bose-Einstein distribution

$$n(E)=\frac{1}{e^{(E-\mu)/T}-1}, \tag{2.5}$$

where μ is now the chemical potential associated with the conserved pion number. Note that μ enters with the same sign for all charge states of the pions. In the literature, the factor $e^{\mu/T}$ is often called a ''fugacity.'' Of course in the true thermodynamic limit where the system has an infinite amount of time to change the number of particles, $\mu=0$. Therefore, a nonvanishing fugacity parameter $\mu\neq 0$ is often referred to as an indication of chemical nonequilibrium. This concept can lead to some confusion, as we shall outline now.

First of all, let us stress the difference between what we shall call *true* number-changing processes, such as

$$\pi\pi\rightleftharpoons\pi\pi\pi\pi, \tag{2.6}$$

and *apparent* number-changing processes, such as

$$\pi\pi\rightleftharpoons\rho. \tag{2.7}$$

As we will demonstrate in the following, the first process drives the fugacity parameter μ to zero, leading to an *absolute* chemical equilibrium. In the second process, on the other hand, the pions are simply ''locked up'' in the ρ meson, but never really disappear. This process ceases to be effective once $2\mu_\pi=\mu_\rho$ with μ_π not necessarily vanishing. Thus, pions and ρ mesons can be chemically equilibrated with each other at any value of μ_π. This condition we will refer to as *relative* chemical equilibrium. Consequently, this process and many others of that kind do not drive the system to *absolute* chemical equilibrium, i.e., $\mu_\pi=0$.

Whenever in the following discussion we refer to a ''chemical potential'' we actually talk about the fugacity parameter μ. Whenever we talk about chemical equilibrium, we mean the *absolute* chemical equilibrium. When particles such as the ρ meson and the pions are in chemical equilibrium with respect to each other, we will talk about a *relative* chemical equilibrium. After these hopefully clarifying remarks let us now turn to the calculation of the chemical relaxation times.

C. Chemical relaxation time for pions

The characteristic time associated with chemical equilibrium is determined by a large number and variety of inelastic processes. The following processes are a subset of possible reactions in hadronic matter which change the number of pions:

$$\text{(a)}\quad \pi+\pi\rightleftharpoons\pi+\pi+\pi+\pi, \tag{2.8}$$

$$\text{(b)}\quad \pi+\pi\rightleftharpoons\rho,$$

$$\pi+\pi+\pi\rightleftharpoons\omega,$$

$$\pi+\rho\rightleftharpoons a_1, \tag{2.9}$$

$$\text{(c)}\quad \pi+\pi\rightleftharpoons\rho+\rho,$$

$$\pi+\pi\rightleftharpoons\pi+\omega,$$

$$\pi+\pi\rightleftharpoons\pi+a_1. \tag{2.10}$$

In order to estimate the characteristic time scales for chemical equilibrium we consider a system slightly out of equilibrium. For this case the distribution function in phase space of the various particles takes the form

$$f(p,x)=\frac{1}{\exp[\beta_\nu(p^\nu-\lambda^\nu)]-1}, \tag{2.11}$$

where p_ν is the four-momentum of the particle. $\lambda_\nu(x)$ and $\beta_\nu(x)$ are four-vectors constructed from the local flow velocity $u_\nu(x)$, the local chemical potential $\mu(x)$, and the inverse local temperature $\beta(x)=1/T(x)$:

$$\lambda_\nu(x)=\mu(x)u_\nu(x), \tag{2.12}$$

$$\beta_\nu(x)=\beta(x)u_\nu(x). \tag{2.13}$$

As explained in the beginning, the nonvanishing chemical potential μ is the parameter which measures to which extent the system deviates from *absolute* chemical equilibrium.

For simplicity we consider hadronic matter in which all thermodynamic variables depend only on time and are uniform in space. The change in particle density (n) is then given by Boltzmann-type rate equations [16]

$$\frac{dn(t)}{dt}=\delta n(R_{\text{gain}}-R_{\text{loss}}), \tag{2.14}$$

where δn is the number of particles changed in the process and $R_{\rm gain}$ and $R_{\rm loss}$ are standard Boltzmann collision integrals for the production and annihilation rates, respectively.

1. Pion gas

To be specific, let us consider first hadronic matter at low temperatures which mainly consists of pions. Since chiral symmetry suppresses the reaction rates for multipion scattering, we consider an inelastic reaction with the minimum number of pions, i.e., the reaction $\pi+\pi\rightleftharpoons\pi+\pi+\pi+\pi$. In this case the gain term, i.e., the term that *increases* the pion number, is associated with the reaction $\pi+\pi\rightarrow\pi+\pi+\pi+\pi$ and the loss term is related to the backwards process. Using the relation for the matrix element $\mathcal{M}$,

$$|\mathcal{M}(\pi\pi\rightarrow\pi\pi\pi\pi)|^2=|\mathcal{M}(\pi\pi\pi\pi\rightarrow\pi\pi)|^2, \quad (2.15)$$

the rate of change for the pion number is given by

$$\frac{dn_\pi(t)}{dt}=2\mathcal{S}\int\frac{d^3p_1}{(2\pi)^3 2E_1}\int\frac{d^3p_2}{(2\pi)^3 2E_2}\cdots\int\frac{d^3p_6}{(2\pi)^3 2E_6}(2\pi)^4\delta^{(4)}(p_1+p_2-p_3-\cdots-p_6)$$
$$\times\sum_{1,2,\ldots,5,6}|\mathcal{M}(\pi_1\pi_2\rightarrow\pi_3\cdots\pi_6)|^2\{f_1(p_1)f_2(p_2)[1+f_3(p_3)]\cdots[1+f_6(p_6)]$$
$$-f_3(p_3)\cdots f_6(p_6)[1+f_1(p_1)][1+f_2(p_2)]\}. \quad (2.16)$$

Here, the pion density $n_\pi(t)$ is the sum over all charge states. The statistical factor $\mathcal{S}$ for the initial and final states is given by 1/2! 4! and the sum is over the isospin degeneracy of all participating particles. In the Maxwell-Boltzmann limit of the Bose-Einstein quantum statistics, we have

$$\frac{dn_\pi}{dt}=2(e^{2\mu_\pi/T}-e^{4\mu_\pi/T})I_0(T), \quad (2.17)$$

where

$$I_0(T)=\mathcal{S}\int\frac{d^3p_1}{(2\pi)^3 2E_1}\int\frac{d^3p_2}{(2\pi)^3 2E_2}\cdots\int\frac{d^3p_6}{(2\pi)^3 2E_6}$$
$$\times(2\pi)^4\delta^{(4)}(p_1+p_2-p_3-\cdots-p_6)$$
$$\times\sum_{1,2,\ldots,5,6}|\mathcal{M}(\pi_1\pi_2\rightarrow\pi_3\cdots\pi_6)|^2 e^{-(E_1+E_2)/T}. \quad (2.18)$$

Notice that the number of pions ceases to change if and only if $\mu_\pi=0$. Thus, the process $\pi+\pi\rightleftharpoons\pi+\pi+\pi+\pi$ drives the system to an *absolute* chemical equilibrium and, therefore, is a true number-changing process according to our previous definition. If we assume that the system is only slightly away from chemical equilibrium, i.e., $\mu_\pi/T\ll 1$, we may expand the exponentials to first order in μ_π/T. Also, in this approximation, for fixed temperature,

$$n_\pi(t)=n_\pi^0\left(1+\frac{\mu_\pi(t)}{T}\right), \quad (2.19)$$

where n_π^0 stands for the equilibrium density. The above rate equation (2.17) then reduces to

$$n_\pi^0\frac{d\mu_\pi}{dt}=-4\mu_\pi I_0(T). \quad (2.20)$$

The solution is given by

$$\mu_\pi(t)=\mu_\pi(0)\exp(-t/\tau_{\rm ch}), \quad (2.21)$$

with

$$\frac{1}{\tau_{\rm ch}}=\frac{4I_0(T)}{n_\pi^0}. \quad (2.22)$$

The above approximations are nothing else but the well-known relaxation time approximation and $\tau_{\rm ch}$ is called the chemical relaxation time.

For pion gas, the relaxation time has been calculated and estimated to be about 40 fm/c with $T=180$ MeV [17]. This is very large compared to the size of the hot matter produced in nucleus-nucleus collisions. This implies that the chemical equilibrium in the reaction $\pi\pi\rightleftharpoons\pi\pi\pi\pi$ would not be reached in the expanding hot hadronic matter consisting of pions only.

2. Resonance gas

In the presence of excited states, i.e., resonances, the number of pions is changed by the decay process of resonances (and vice versa), e.g., $\rho\rightleftharpoons\pi\pi$, $\omega\rightleftharpoons\pi\pi\pi$, $a_1\rightleftharpoons\pi\rho$, and inelastic scattering such as $\rho\rho\rightleftharpoons\pi\pi$, $\pi\omega\rightleftharpoons\pi\pi$, $\pi a_1\rightleftharpoons\pi\pi$, etc.

(a) Resonance decays. First we consider resonance decays. In this case the relaxation time will be inversely proportional to the decay width. Specifically, in the case of $\rho\rightleftharpoons\pi\pi$ we have

$$\frac{dn_\pi(t)}{dt}=2(e^{\mu_\rho/T}-e^{2\mu_\pi/T})I_0(\rho\rightleftharpoons\pi\pi;T). \quad (2.23)$$

$I_0(\rho\rightleftharpoons\pi\pi;T)$ can be related to the decay width of the ρ via

$$I_0(\rho\rightleftharpoons\pi\pi;T)=\sum_\rho\int\frac{d^3p_\rho}{(2\pi)^3}\frac{E_\rho}{m_\rho}\Gamma(p_\rho)f_\rho(p_\rho)\approx\overline{\Gamma}n_\rho^0(T), \quad (2.24)$$

where the sum is over spin and isospin of vector mesons. $\overline{\Gamma}_\rho$ is the decay width of neutral vector mesons and n_ρ^0 indicates the equilibrium density summed over all spin and isospin states.

Notice that from Eq. (2.23) the process $\rho \rightleftharpoons \pi\pi$ ceases to change the number of pions once $\mu_\rho = 2\mu_\pi$. This may very well happen at a finite value μ_π. Consequently this process does not drive the system into *absolute* chemical equilibrium, as we have defined it. It rather ensures a *relative* chemical equilibrium between ρ mesons and pions, which is characterized by the condition $\mu_\rho = 2\mu_\pi$. Following our definitions, the process $\rho \rightleftharpoons \pi\pi$ is an apparent number-changing one, since it only shuffles pions back and forth from the ρ resonance. The fact that the pion chemical potential can take on a finite value means nothing else than the conservation of the pion number in this type of process.

Expanding the distribution functions around the *relative* chemical equilibrium , one can again derive a relaxation time $\tau_{\rm ch}^{\rm rel}$, which is a measure of how fast the *relative* chemical equilibrium between pions and ρ mesons is reached. Following the steps of the previous section one finds

$$\tau_{\rm ch}^{\rm rel} = \frac{1}{\overline{\Gamma}}\left(\frac{n_\pi^0}{n_\pi^0 + 4n_\rho^0}\right) \approx 1(0.4) \quad \text{fm}/c, \tag{2.25}$$

at $T = 150(180)$ MeV. This is very short, and to a good approximation we can assume that pions and ρ meson are always in *relative* chemical equilibrium.

The same conclusion holds for the decay $a_1 \to \pi\rho$ since $\Gamma_{a_1 \to \rho\pi} = 400$ MeV. Thus we have $\mu_{a_1} = \mu_\pi + \mu_\rho = 3\mu_\pi$ where we use $\mu_\rho = 2\mu_\pi$. However, the decay rate for omega mesons into three pions is too small in order to reach *relative* chemical equilibrium.

(b) Inelastic scattering. Next, we consider the inelastic collisions involving resonances such as $\pi + \pi \rightleftharpoons \rho + \rho$, $\pi + \omega \rightleftharpoons \pi + \pi$, and $\pi + a_1 \rightleftharpoons \pi + \pi$. Again, the rate of change of pion density is given by (here in case of $\pi + \pi \rightleftharpoons \rho + \rho$)

$$\frac{dn_\pi}{dt} = 2(e^{2\mu_\rho/T} - e^{2\mu_\pi/T}) I_0(\pi + \pi \rightleftharpoons \rho + \rho; T). \tag{2.26}$$

As long as the process $\rho \rightleftharpoons \pi\pi$ is fast compared to the one we are considering here, we can, to a good approximation assume that pions and ρ mesons are in *relative* chemical equilibrium, i.e., $\mu_\rho = 2\mu_\pi$. With this replacement, the above rate equation (2.26) becomes similar to Eq. (2.17) and, hence, the chemical relaxation time is given by [see Eq. (2.22)]

$$\frac{1}{\tau_{\rm ch}} = \frac{4I_0(\pi + \pi \rightleftharpoons \rho + \rho; T)}{n_\pi^0}. \tag{2.27}$$

The same arguments hold for the process $\pi + a_1 \rightleftharpoons \pi + \pi$, whereas the approximation will be not valid in case of $\pi + \omega \rightleftharpoons \pi + \pi$. For the reactions involving ω mesons we assume $\mu_\omega \approx 0$ to estimate the corresponding contribution to the chemical relaxation time of pions.

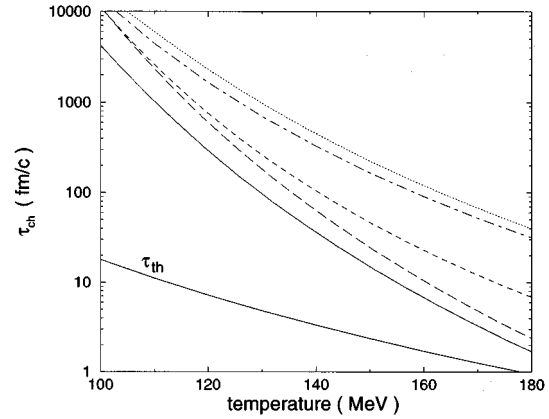

FIG. 1. Chemical relaxation time of pions in hot hadronic matter. The reactions $\rho\rho \leftrightarrow \pi\pi$ (dashed curve), $\pi\omega \leftrightarrow \pi\pi$ (dot-dashed curve), $\pi a_1 \leftrightarrow \pi\pi$ (long-dashed curve), and $\pi\pi\pi\pi \leftrightarrow \pi\pi$ (dotted curve) are considered. The solid curve represents the total relaxation time. These results are compared with the thermal relaxation time $\tau_{\rm th}$ obtained from Eq. (2.4).

In order to evaluate the relevant collision integrals, hadronic cross sections have been calculated from an effective chiral Lagrangian with vector and axial vector mesons. The details are given in Appendix A. All processes included in the calculation are summarized and results for invariant amplitudes are presented in Appendix B. To take into account the off-energy-shell effects we introduce form factors in the calculation of the cross section. The standard way to accomplish this is to insert a monopole form factor at each vertex in a t-channel diagram,

$$F_\alpha = \frac{\Lambda^2 - m_\alpha^2}{\Lambda^2 - t}, \tag{2.28}$$

where α indicates a species for the exchanged particle. We take a value of $\Lambda = 1.7$ GeV for $\rho\pi\pi$ vertices in ρ exchange reactions [18] and of m_ρ in pion exchange processes. $\Lambda = m_{a_1}$ and 1.7 GeV are taken for $a_1\pi\rho$ vertices and $\omega\rho\pi$ vertices, respectively.

In Fig. 1 we show the chemical relaxation times for each process as a function of temperature. For comparison the chemical relaxation time corresponding to the reaction $\pi\pi\pi\pi \rightleftharpoons \pi\pi$ is also shown [17]. The total relaxation time is determined by including all true pion-number-changing processes $\pi + \pi \rightleftharpoons \rho + \rho$, $\pi + \pi \rightleftharpoons \pi + a_1$, and $\pi + \pi \rightleftharpoons \pi + \pi + \pi + \pi$. The result is given by the solid curve. As a result of the hadronic resonances, the resulting relaxation time is almost an order of magnitude shorter than that previously obtained within chiral perturbation theory [17]. We find that the relaxation time is about 1.5 fm/c at $T \sim 180$ MeV and increases to about 15 fm/c at $T = 150$ MeV.

At a temperature of $T \simeq 160$ MeV the total relaxation time is about 7 fm/c, which is comparable to typical system sizes created in ultrarelativistic heavy-ion collisions involving heavy nuclei such as lead. However, the corresponding temperature, for which the thermal relaxation time assumes the same value of $\tau_{\rm th} = 7$ fm/c, is considerably low, namely, about 120 MeV. From these numbers we expect that even with the inclusion of the resonance chemical freeze-out takes

place before the thermal one. Moreover, the above estimate has assumed that the resonances are formed instantaneously. Thus, the chemical relaxation time may be slightly larger once the formation of the resonances is taken into account properly.

3. Absorption on baryons

Next, we take into account the pion-number-changing processes involving baryons. The dominant contributions come from low-lying baryons, like nucleons $N(938)$ and $\Delta(1236)$. Since the Δ resonance decays into $N\pi$ with width $\Gamma_{\Delta N\pi}=120$ MeV, we expect that there will be a *relative* chemical equilibrium with respect to the reaction $\Delta\rightarrow N\pi$ with $\mu_\Delta=\mu_B+\mu_\pi$. Here μ_B indicates the baryon chemical potential, associated with the conservation of the baryon number.

There are also inelastic, i.e., true pion-number-changing, reactions including baryon resonances, such as $N\Delta\rightleftharpoons NN$. To estimate the characteristic time scale for the baryon-induced inelastic collisions we use a phenomenological parametrization for the isospin-averaged $N\Delta\rightarrow NN$ cross section [19],

$$\sigma(N\Delta\rightarrow NN)=(p_f^2/p_i^2)\tfrac{1}{8}\sigma(\sqrt{s}), \tag{2.29}$$

where p_f is the momentum in the final NN channel and

$$\sigma(\sqrt{s})=\frac{20\times(\sqrt{s}-2.015)^2}{0.015+(\sqrt{s}-2.015)^2}. \tag{2.30}$$

Here $\sqrt{s}$ is in GeV, σ in mb. Then the time scale $\tau_{\rm ch}$ is given by

$$\frac{1}{\tau_{\rm ch}}=\frac{1}{n_\pi^0}e^{2\mu_B/T}I_B(T), \tag{2.31}$$

where we use $\mu_\Delta=\mu_B+\mu_\pi$ and

$$I_B(T)=\int\frac{d^3p_N}{(2\pi)^3}\int\frac{d^3p_\Delta}{(2\pi)^3}\sum_{1,2}\sigma(N\Delta\rightarrow NN)v_{12}e^{-\beta E_N-\beta E_\Delta}. \tag{2.32}$$

Here the sum is over the spin and isospin for the initial particles.

Results are shown in Fig. 2. We use $\mu_B=176$, 223, 278, and 516 MeV for the baryon chemical potential which are obtained from the analyses of SPS-energy data on strange baryon and antibaryon production [8,11] and of AGS-energy reactions [7]. The time scale turns out to be about ~ 100 fm/c even at $T=180$ MeV except for the AGS experiments. This is too large to change the number of pions in expanding hot hadronic matter. For AGS experiments with $\mu_B=516$ MeV we find that $\tau_{\rm ch}\sim 10$ fm/c at $T\sim 160$ MeV. This implies that the baryon effect might be relevant for AGS experiments but negligible in case of SPS experiments. In the following we therefore ignore the corrections due to the presence of baryons.

Including the finite width of delta resonance in the calculation of the cross section, $\sigma(N\Delta\rightarrow NN)$ [20], the relaxation time is slightly reduced. We show the correction due to a finite delta width in case of AGS experiments by a dot-dashed curve in Fig. 2. The effect is, however, too small to change any conclusion.

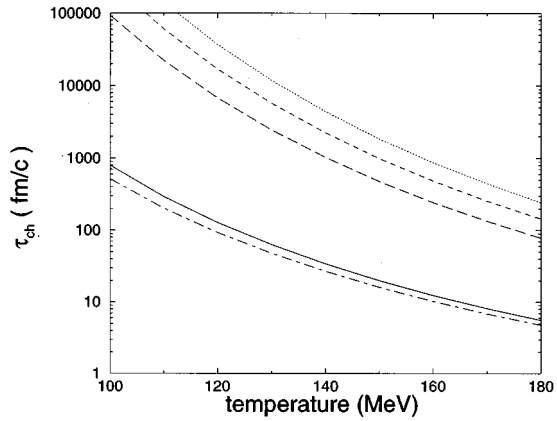

FIG. 2. Contribution of baryon-involved reactions to the chemical relaxation time of pions in hot hadronic matter. Results are obtained with $\mu_B=176$ MeV (dotted curve, SPS), 223 MeV (dashed curve, SPS), 278 MeV (long-dashed curve, SPS), and $\mu_B=516$ MeV (solid curve, AGS). The dot-dashed curve is obtained with finite width of Δ resonances with $\mu_B=516$ MeV.

III. CHEMICAL EQUILIBRIUM WITH FINITE PION CHEMICAL POTENTIAL

So far we have considered the characteristic time scale for chemical equilibration of pions when the system is slightly out of chemical equilibrium. This is the case either when the hadronic system evolves from a fully equilibrated quark-gluon plasma phase and hadronizes without any changes in chemical properties or when the hadronic system directly is produced in thermodynamic equilibrium state. However, if the system is out of chemical equilibrium initially, the reaction rate for the pion-number-changing processes will be affected by the finite pion chemical potential.

We therefore extend the previous definition for the chemical relaxation time to the case with finite chemical potential and define

$$\frac{1}{\tau_{\rm ch}}\equiv\frac{-1}{[n(T,\mu_\pi)-n^0(T)]}\frac{dn(T,\mu_\pi)}{dt}, \tag{3.1}$$

which is the ratio of the pion-number-changing rate over the the excess (or lack) of pions as compared to equilibrium. In the limit of vanishing chemical potential, $\mu_\pi\rightarrow 0$, the resulting chemical relaxation time coincides with that derived in the previous section.

A. Chemical relaxation time of pions: Out of equilibrium

In the previous section we found that for a pure pion gas the chemical equilibration rate evaluated near chemical equilibrium is too long to be effective. If the system is far away from chemical equilibrium, then the annihilation (production) reaction rates depend on the value of the chemical potential. For the reaction $\pi\pi\pi\pi\rightarrow\pi\pi$ with a finite chemical potential of pions, the chemical relaxation time, Eq. (3.1), is given by

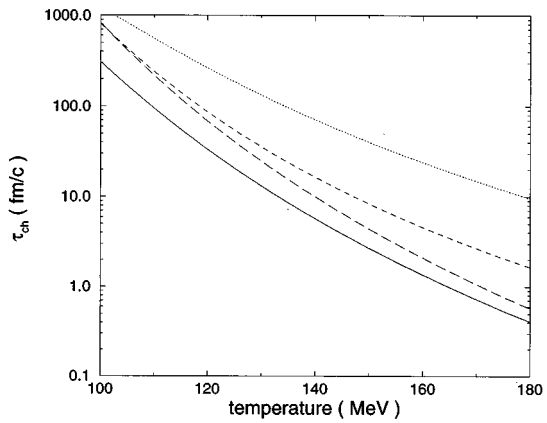

FIG. 3. Chemical relaxation time of pions in hot hadronic matter with finite pion chemical potential. The contributions from the reaction $\rho\rho\leftrightarrow\pi\pi$ (dashed curve), $\pi a_1\leftrightarrow\pi\pi$ (long-dashed curve), and $\pi\pi\pi\pi\leftrightarrow\pi\pi$ (dotted curve) are shown. The solid curve is for the total relaxation time. The results are obtained with $\mu_\pi=100$ MeV.

$$\frac{1}{\tau_{\rm ch}^{\pi}}=-\frac{2}{n_\pi^0(T)}e^{2\mu_\pi/T}(1-e^{2\mu_\pi/T})\times I_0(\pi\pi\pi\pi\rightleftharpoons\pi\pi;T)/(e^{\mu_\pi/T}-1), \tag{3.2}$$

where we take the Boltzmann approximation for the distribution of pions. The calculated chemical relaxation time is shown as dotted line in Fig. 3 for $\mu_\pi=100$ MeV. When the system is out of equilibrium the number-changing process becomes considerably faster — about a factor of 5 at $T=150$ MeV — than in the previous case where the system was near equilibrium (note the different scale on the y axis of Fig. 3). However, the reaction rate is still large compared to the size of the system, $\tau_{\rm ch}^{\pi}\sim 10$ fm/c at $T=180$ MeV. Thus, in a hadronic system consisting of only pions, the number of pions ceases to change at the early stage of the expansion even if the system is out of equilibrium at the beginning of the evolution.

Once we include resonances, additional processes help to change the pion number. Again we assume that decay processes such as $\rho\rightleftharpoons\pi\pi$ and $a_1\rightleftharpoons\pi\rho$ are fast enough to maintain the *relative* chemical equilibrium even if pions have a finite chemical potential. From Eq. (2.14) we can see that the pion number is not changed by these reactions. The pion number will be changed, however, by reactions such as $\rho\rho\rightarrow\pi\pi$ and $\pi a_1\rightarrow\pi\pi$; these reactions actually mean that four pions decay into two pions. The chemical relaxation time for the corresponding reactions is given by

$$\frac{1}{\tau_{\rm ch}^{\pi}}=-\frac{2}{n_\pi^0(T)}(e^{2\mu_\pi/T}-e^{2\mu_\rho/T})\times I_0(\rho\rho\rightleftharpoons\pi\pi;T)/(e^{\mu_\pi/T}-1), \tag{3.3}$$

with $\mu_\rho=2\mu_\pi$. We also get a similar relation for the $\pi a_1\rightarrow\pi\pi$,

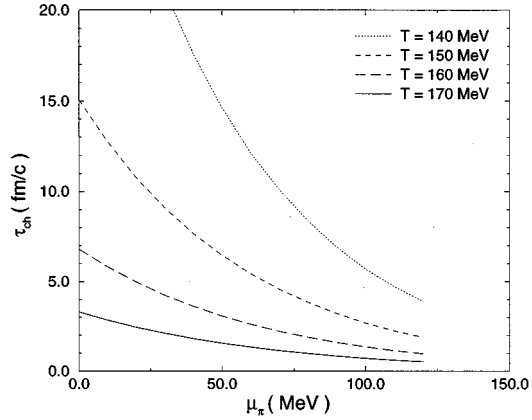

FIG. 4. Chemical relaxation time of pions in hot hadronic matter as a function of pion chemical potential. We consider four different temperatures, from top, $T=140$, 150, 160, 170 MeV.

$$\frac{1}{\tau_{\rm ch}^{\pi}}=-\frac{2}{n_\pi^0(T)}(e^{2\mu_\pi/T}-e^{(\mu_\pi+\mu_{a_1})/T})\times I_0(\pi a_1\rightleftharpoons\pi\pi;T)/(e^{\mu_\pi/T}-1), \tag{3.4}$$

where $\mu_{a_1}=3\mu_\pi$.

We show the relaxation time with $\mu_\pi=100$ MeV in Fig. 3. The total chemical relaxation time for $\pi\pi\pi\pi\rightleftharpoons\pi\pi$ is given by the sum for all possible channels. With a finite chemical potential of pions, the chemical relaxation time of pions now becomes short compared to the size of the system. Thus the number of pions would be changed in hot hadronic matter even near the thermal freeze-out temperature. The oversaturated pion number will be reduced mainly by the reactions $\rho\rho\rightarrow\pi\pi$ and $\pi a_1\rightarrow\pi\pi$. Especially axial vector mesons very easily interact with pions and annihilate into two pions. However, we should note that the thermal freeze-out temperature is also reduced when we include a finite pion chemical potential [14].

With a nonzero pion chemical potential one also expects an oversaturation of vector and axial vector mesons with the relation $\mu_\rho=2\mu_\pi$ and $\mu_{a_1}=3\mu_\pi$, respectively. The above result, of course, implies that also the number of vector and axial vector mesons changes as quickly as that of the pions.

In Fig. 4 we show how the total chemical relaxation time is changed with pion chemical potential at fixed temperature. Even at $T=150$ MeV, the pion relaxation time is comparable to the size of the hot system as long as the pions have a finite chemical potential, $\tau_{\rm ch}\approx 7$ fm/c at $\mu_\pi=50$ MeV. If the hadronic system is produced out of equilibrium, for example, with $\mu_\pi=100$ MeV, the excess of pions will be reduced by the inelastic reactions involving vector and axial vector mesons. These number-changing processes will lead to the decrease of the pion chemical potential and finally cease to be effective as the chemical potential is reduced below a certain value. Therefore, given a freeze-out temperature of about 150 MeV and 7 fm for the size of the system, we would expect the pion chemical potential not to exceed a value of $\mu_\pi\simeq 50$ MeV.

B. Chemical relaxation time of pions: In equilibrium

In the previous section we have demonstrated that the chemical relaxation time depends on both the temperature and the chemical potential. In order to give a realistic estimate of the chemical relaxation time, one thus needs to know the chemical potential as a function of temperature. The correct treatment, of course, requires the complete solution of all kinetic equations including the expansion of the system. This is best done in a transport approach and will be addressed in a separate work. In order to give a rough estimate let us separate the problem into two pieces. First of all, we determine the chemical potential as a function of temperature, assuming the *absence* of any number-changing processes. Given that, we can then evaluate the chemical relaxation time using our previous results.

In order to determine the chemical potential as a function of temperature, we assume that the system initially (after hadronization) is in chemical equilibrium. We furthermore ignore all true number changing processes. In this case we have only two possible reactions in the hadronic phase: elastic pion scattering which maintains the thermal equilibrium and the decay of the excited states, e.g., $\rho\rightarrow\pi\pi$ and $a_1\rightarrow\pi\rho$. The local configuration of pions is then described by temperature and a single chemical potential μ.

Since the system still remains in thermal equilibrium, the state can be characterized by a maximum of the entropy consistent with the conservation laws of energy and momentum and of relevant particle numbers. Since we neglect dissipative, i.e., pion-number-changing, processes, this implies that entropy as well as the pion number is conserved in the expansion. Thus one can assume that the ratio of the effective pion number density $\overline{n}_\pi = n_\pi + 2n_\rho + 3n_{a_1} + \cdots$ to entropy density s remains constant during the expansion after hadronization until freeze-out,

$$\frac{s}{\overline{n}_\pi} = \text{const.} \tag{3.5}$$

As a result of keeping $s/\overline{n}_\pi$ constant, the chemical potential will rise. This is so because of the overpopulation of pionic states due to the decay of the resonances. It has been estimated that the pion chemical potential is about 86 MeV at the freeze-out temperature $T_f = 100$ MeV [21]. To be specific, we assume that the particles are distributed according to

$$f_i = \frac{g_i}{\exp(E_i - \mu_i)/T - 1}, \tag{3.6}$$

where $i = \pi, \rho, a_1, \ldots$ and g_i is the spin and isospin degeneracy factor and $E_i = \sqrt{p^2 + m_i^2}$. The entropy density is given by

$$s = \left.\frac{\partial P}{\partial T}\right|_{\mu=\text{const}}, \tag{3.7}$$

where the pressure is

$$P = -T\sum_i g_i \int \frac{d^3p}{(2\pi)^3} \ln\left\{1 - \exp\left(\frac{\mu_i - E_i}{T}\right)\right\}. \tag{3.8}$$

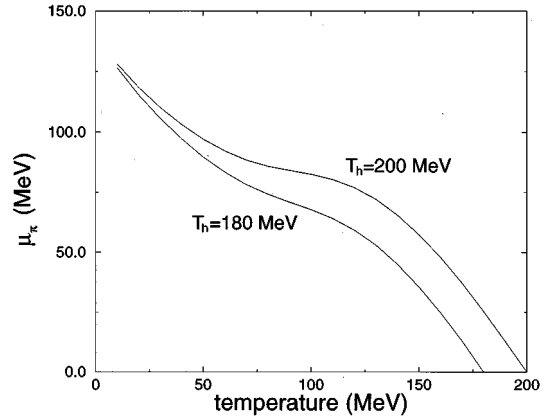

FIG. 5. Temperature dependence of the pion chemical potential: We assume two different initial (hadronization) temperatures $T_h = 180$ (lower curve) and 200 MeV (upper curve).

Assuming that the ratio of entropy density of the system to effective pion number density is constant throughout expansion, we can obtain the temperature dependence of the pion chemical potential as shown in Fig. 5 [21]. Here we take two different initial (hadronization) temperatures $T_h = 180$ and 200 MeV, where the chemical potential is assumed to be zero, $\mu_\pi = 0$.

With the temperature dependence of the pion chemical potential we can calculate the total chemical relaxation time based on the reactions $\pi\pi\pi\pi\rightarrow\pi\pi$, $\rho\rho\rightarrow\pi\pi$, and $a_1\pi\rightarrow\pi\pi$. We show the result in Fig. 6. At the initial temperature we, of course, have the same value for the chemical relaxation time as that obtained in the limit $\mu_\pi\rightarrow 0$. As the system expands and pions develop the chemical potential the relaxation time become shorter than that obtained near equilibrium (as shown by dotted line). We find that the τ_{ch} is reduced by half at $T = 150$ MeV ($\tau_{\text{ch}} \sim 7$ fm/c) due to the pion chemical potential. However, even with the induced pion chemical potential the chemical relaxation time is considerably larger than the thermal relaxation time at the same temperature.

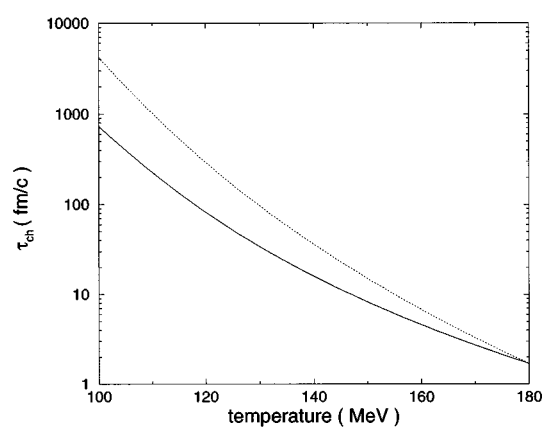

FIG. 6. Chemical relaxation time of pions (solid curve) with pion chemical potential shown in Fig. 3. Here we assume that $T_h = 180$ MeV. The result is compared with the one obtained with $\mu_\pi = 0$ (dotted curve).

IV. SUMMARY

We have studied the thermal and chemical relaxation time scales of pions in hot hadronic matter with an effective chiral Lagrangian. From the explicit calculation we show that pions in hot hadronic matter are in a phase where elastic collisions rates are very fast compared to typical expansion rates of the system. For chemical equilibration the dominant contribution comes from the inelastic collision involving a_1 mesons. Comparing with previous calculations [17] based on chiral perturbation theory, the inclusion of the resonances has reduced the chemical relaxation time by about a factor of 10. When we neglect the formation time of these resonances, the resulting chemical relaxation time of pions is 7 fm/c at $T=160$ MeV. This value is comparable to the size of the hot system produced by the collision of large nuclei.

Given a system size of 5–10 fm we obtain a thermal freeze-out temperature which is small compared to those extracted from experiments [6,11]. This might be due to flow effects which lead to smaller effective system sizes. If we take the thermal freeze-out temperature to be about 150 MeV, then the freeze-out size of the system would be 2–3 fm. On the other hand, the chemical freeze-out temperature for a system of this size would be $T=180$ MeV. This implies that chemical freeze-out of pions happens at considerably higher temperatures than thermal freeze-out. This result is somewhat at variance with the findings of [8,9], where pion spectra and particle abundances could be reproduced, assuming the same freeze-out conditions. In order to properly assess the magnitude and importance of this discrepancy, a detailed transport calculation including all the number-changing processes presented here is needed.

We also have studied the effect of baryons on the chemical relaxation time of pions. Since the effect of baryons is suppressed by their large mass, we consider only low-lying baryons $N(938)$ and $\Delta(1236)$. To estimate the relaxation time we use the phenomenological cross section for $NN \rightleftharpoons N\Delta$. The effect of baryons is very small and can be neglected in SPS experiments. However, it becomes important in AGS experiments where the baryon chemical potential is much larger than that in the SPS experiments.

We have extended the definition for the chemical relaxation time to a system of pions out of equilibrium with $\mu_\pi \neq 0$. At $T=150$ with $\mu_\pi=50$ MeV the relaxation time is about 7 fm/c which is certainly comparable to the system size. Thus even at $T=150$ MeV it is possible that the number of pions will be changed by the inelastic reactions involving vector and axial vector mesons as long as $\mu_\pi \geqslant 50$ MeV.

In order to make contact with reality, we have determined the pion chemical potential as a function of temperature, assuming isentropic expansion, while ignoring number-changing processes. Based on this relation, we could give a somewhat more realistic estimate of the actual chemical relaxation time. As the system expands and pions develop the chemical potential the relaxation time becomes shorter than that obtained near equilibrium. If we take the size of the system as about 5–10 fm, the inelastic reactions are effective at $T=140$–180 MeV and reduce pion chemical potentials. We therefore expect that the chemical potential at freeze-out will be smaller than the value which has been obtained without taking number-changing processes into account.

In conclusion, we predict a considerable difference between the chemical and thermal freeze-out temperatures. The extent which this is reflected in the data needs to be investigated within a transport calculation. At the same time, a buildup of a pion chemical potential larger than 100 MeV would be very difficult to understand in hot hadronic matter with a size of about 5–10 fm.

Future work will concentrate on a transport theoretical calculation of the chemical equilibration. We also plan to extented the present study to include reactions involving strange particles.

ACKNOWLEDGMENTS

This work was supported by the Director, Office of Energy Research, Office of High Energy and Nuclear Physics, Division of Nuclear Physics, Division of Nuclear Sciences, of the U.S. Department of Energy under Contract No. DE-AC03-76SF00098.

APPENDIX A: EFFECTIVE CHIRAL LAGRANGIAN

We consider an effective chiral Lagrangian with vector and axial vector meson fields which are introduced as massive Yang-Mills fields [22],

$$\begin{aligned}\mathcal{L}=&\tfrac{1}{4}f_\pi^2\mathrm{Tr}[D_\mu U D^\mu U^\dagger]+\tfrac{1}{4}f_\pi^2\mathrm{Tr}M(U+U^\dagger-2)\\&-\tfrac{1}{2}\mathrm{Tr}[F^L_{\mu\nu}F^{L\mu\nu}+F^R_{\mu\nu}F^{R\mu\nu}]+m_0^2\mathrm{Tr}[A^L_\mu A^{L\mu}+A^R_\mu A^{R\mu}]\\&-i\xi\mathrm{Tr}[D_\mu U D_\nu U^\dagger F^{L\mu\nu}+D_\mu U^\dagger D_\nu U F^{R\mu\nu}]\\&+\sigma\mathrm{Tr}[F^L_{\mu\nu}UF^{R\mu\nu}U^\dagger],\end{aligned}\tag{A1}$$

where U is related to the pseudoscalar fields ϕ by

$$U=\exp\left[i\sqrt{\frac{2}{f_\pi}}\phi\right],\quad \phi=\sum_{a=1}^{3}\phi_a\frac{\tau_a}{\sqrt{2}},\tag{A2}$$

and $A^L_\mu(A^R_\mu)$ are left- (right-) handed vector fields. The covariant derivative acting on U is given by

$$D_\mu U=\partial_\mu U-igA^L_\mu U-igUA^R_\mu,\tag{A3}$$

and $F^L_{\mu\nu}(F^R_{\mu\nu})$ is the field tensor of left- (right-) handed vector fields. The A^L_μ and A^R_μ can be written in terms of vector (V_μ) and axial vector fields (A_μ) as

$$A^L_\mu=\tfrac{1}{2}(V_\mu-A_\mu),\quad A^R_\mu=\tfrac{1}{2}(V_\mu+A_\mu).\tag{A4}$$

With parameters $g=10.3063$, $\sigma=0.3405$, and $\xi=0.4473$ [23] we can well describe the properties of vector and axial vector mesons.

From the Lagrangian we have

$$\mathcal{L}^{(3)}_{V\phi\phi}=\frac{ig}{2}\mathrm{Tr}\partial_\mu\phi[V^\mu,\phi]+\frac{ig\delta}{2m_V^2}\mathrm{Tr}(\partial_\mu V_\nu-\partial_\nu V_\mu)\partial^\mu\phi\partial^\nu\phi,$$

$$\mathcal{L}^{(3)}_{VVV}=\frac{ig}{2}\mathrm{Tr}(\partial_\mu V_\nu-\partial_\nu V_\mu)V^\mu V^\nu,$$

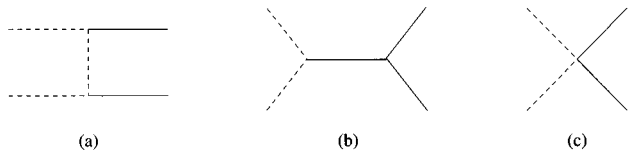

FIG. 7. Diagrams for the reactions $\pi^+ + \pi^- \to \rho^+ + \rho^-$ and $\pi^+ + \pi^0 \to \rho^+ + \rho^0$. Dashed line and solid line indicate the pion and ρ meson, respectively.

$$\mathcal{L}^{(3)}_{VA\phi} = \frac{ig}{2}\frac{1}{f_\pi}\{\eta_1 \mathrm{Tr}(\partial_\mu V_\nu - \partial_\nu V_\mu)[A^\mu, \partial^\nu \phi] + \eta_2 \mathrm{Tr}(\partial_\mu A_\nu - \partial_\nu A_\mu)[\partial^\mu V^\nu, \phi]\}, \tag{A5}$$

where δ, η_1, and η_2 are given by the parameters in the Lagrangian and have the values 0.347, 0.279, and 0.060, respectively.

For the four-point vertex we have

$$\begin{aligned}\mathcal{L}^{(4)}_{VV\phi\phi} = &-\frac{1}{8}g^2 \mathrm{Tr}[V_\mu, \phi]^2 + \frac{c_1}{f_\pi^2}\mathrm{Tr}[(\partial_\mu V_\nu - \partial_\nu V_\mu)\phi \\ &\times(\partial^\mu V^\nu - \partial^\nu V^\mu)\phi - (\partial_\mu V_\nu - \partial_\nu V_\mu)^2 \phi^2] \\ &+ \frac{c_2}{f_\pi^2}\mathrm{Tr}[(\partial_\mu V_\nu - \partial_\nu V_\mu)(\partial^\mu \phi[V^\nu, \phi] \\ &+ [V^\mu, \phi]\partial^\nu \phi)] + \frac{c_2}{f_\pi^2}\mathrm{Tr}[V_\mu, V_\nu]\partial^\mu \phi \partial^\nu \phi,\end{aligned} \tag{A6}$$

and also have

$$\begin{aligned}\mathcal{L}^{(4)}_{A\phi^3} = &\frac{d_1}{f_\pi}\mathrm{Tr} A_\mu(\phi^2 \partial^\mu \phi - 2\phi \partial^\mu \phi \phi + \partial^\mu \phi \phi^2) \\ &+ \frac{d_2}{f_\pi^3}\mathrm{Tr}[A_\mu, \partial_\nu \phi][\partial^\mu \phi, \partial^\nu \phi] + \frac{d_3}{f_\pi^3}\mathrm{Tr}(\partial_\mu A_\nu - \partial_\nu A_\mu) \\ &\times(\partial^\mu \phi \partial^\nu \phi \phi - \phi \partial^\mu \phi \partial^\nu \phi),\end{aligned} \tag{A7}$$

where c's and d's are given by the parameters in the Lagrangian. With parameters given in Ref. [23] we have the values 0.00497 and -0.00408 for c_1 and c_2, respectively, and $d_1 = -2.08$, $d_2 = 0.078$, and $d_3 = -0.0147$.

We also include the gauged Wess-Zumino term in the effective Lagrangian to describe the non-Abelian anomaly structure of QCD [24], which leads to an anomalous interaction among a pseudoscalar meson and two vector mesons,

$$\mathcal{L}_{VVP} = -\frac{3g^2}{16\sqrt{2}\pi^2 f_\pi}\epsilon^{\mu\nu\alpha\beta}\mathrm{Tr}(\partial_\mu V_\nu \partial_\alpha V_\beta P), \tag{A8}$$

where $\epsilon^{\mu\nu\alpha\beta}$ is the antisymmetric Levi-Cività tensor with $\epsilon^{0123} = 1$. From Eq. (A8) we have

$$\mathcal{L}_{\omega\pi\rho} = -g_\omega \epsilon^{\mu\nu\alpha\beta}\partial_\mu \omega_\nu \partial_\alpha \rho_\beta \cdot \pi, \tag{A9}$$

with

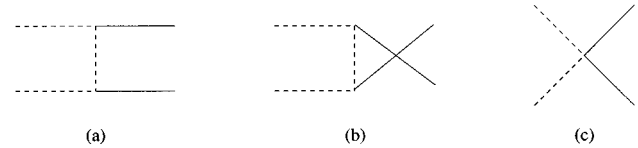

FIG. 8. Same as Fig. 7 for the reactions $\pi^+ + \pi^- \to \rho^0 + \rho^0$ and $\pi^0 + \pi^0 \to \rho^+ + \rho^-$.

$$g_\omega = \left(\frac{3g^2}{16\pi^2 f_\pi}\right). \tag{A10}$$

APPENDIX B: INELASTIC CROSS SECTION

In this appendix we summarize the invariant matrix element for each inelastic collision considered in Sec. II C. The interaction for each process is obtained from the effective Lagrangian.

1. $\pi + \pi \to \rho + \rho$

a. $\pi^+ + \pi^- \to \rho^+ + \rho^-$, $\pi^+ + \pi^0 \to \rho^+ + \rho^0$

The related diagrams are shown in Fig. 7. The explicit expression for the invariant matrix element for each reaction is given by

$$\mathcal{M}^{(a)} = i\left[\frac{g}{\sqrt{2}}\left(1 - \frac{\delta}{2}\right)\right]^2 \frac{4p_{1\mu}p_{2\nu}}{(p_1 - p_3)^2 - m_\pi^2}\epsilon^\mu_\rho(p_3)\epsilon^\nu_\rho(p_4), \tag{B1}$$

$$\begin{aligned}\mathcal{M}^{(b)} = i\left(\frac{g}{\sqrt{2}}\right)^2 &\frac{1}{(p_1 + p_2)^2 - m_\rho^2}\left(1 - \frac{\delta}{2m_\rho^2}(p_1 + p_2)^2\right) \\ &\times[(p_1 - p_2)\cdot(p_3 - p_4)g_{\mu\nu} + 2p_{4\mu}(p_{1\nu} - p_{2\nu}) \\ &- 2(p_{1\mu} - p_{2\mu})p_{3\nu}]\epsilon^\mu_\rho(p_3)\epsilon^\nu_\rho(p_4),\end{aligned} \tag{B2}$$

$$\begin{aligned}\mathcal{M}^{(c)} = i\left(\frac{g}{\sqrt{2}}\right)^2 &\left\{\left[1 + 4\frac{c_1}{f_\pi^2}p_3 \cdot p_4 - 2\frac{c_2}{f_\pi^2}(p_1 \cdot p_4 + p_2 \cdot p_3)\right]g_{\mu\nu}\right. \\ &- 4\frac{c_1}{f_\pi^2}p_{4\mu}p_{3\nu} + 2\frac{c_2}{f_\pi^2}(p_{4\mu}p_{1\nu} + p_{2\mu}p_{3\nu} \\ &\left. - p_{1\mu}p_{2\nu} + p_{2\mu}p_{1\nu})\right\}\epsilon^\mu_\rho(p_3)\epsilon^\nu_\rho(p_4),\end{aligned} \tag{B3}$$

where c_1 and c_2 are given in the previous section.

The invariant scattering matrix element is then given by the sum as

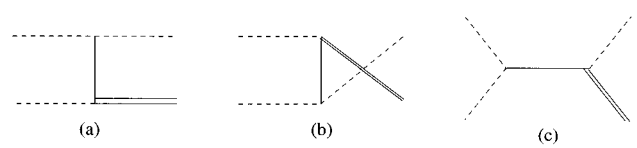

FIG. 9. Diagrams for the reaction $\pi\omega \to \pi\pi$. Dashed line, solid line, and double solid line indicate the pion, ρ meson, and ω meson, respectively.

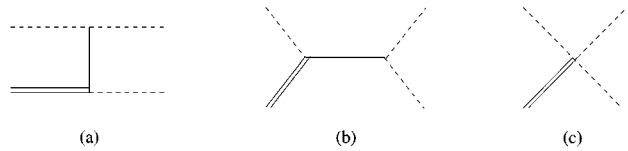

FIG. 10. Diagrams for the reactions $\pi^+ + a_1^0 \to \pi^0 + \pi^+$ and $\pi^+ + a_1^- \to \pi^+ + \pi^-$ Dashed line, solid line, and double solid line indicate the pion, ρ meson, and a_1 meson, respectively.

$$\mathcal{M}(\pi^+ + \pi^- \to \rho^+ + \rho^-) = \mathcal{M}(\pi^+ + \pi^0 \to \rho^+ + \rho^0) = \mathcal{M}^{(a)} + \mathcal{M}^{(b)} + \mathcal{M}^{(c)}. \tag{B4}$$

b. $\pi^+ + \pi^- \to \rho^0 + \rho^0$, $\pi^0 + \pi^0 \to \rho^+ + \rho^-$

The related diagrams are shown in Fig. 8. The explicit expression for the invariant matrix element for each reaction is given by

$$\mathcal{M}^{(a)} = \frac{-i}{2}\left[\frac{g}{\sqrt{2}}\left(1 - \frac{\delta}{2}\right)\right]^2 \frac{4p_{1\mu}p_{2\nu}}{(p_1 - p_3)^2 - m_\pi^2}\epsilon_\rho^\mu(p_3)\epsilon_\rho^\nu(p_4), \tag{B5}$$

$$\mathcal{M}^{(b)} = \frac{-i}{2}\left[\frac{g}{\sqrt{2}}\left(1 - \frac{\delta}{2}\right)\right]^2 \frac{4p_{2\mu}p_{1\nu}}{(p_3 - p_2)^2 - m_\pi^2}\epsilon_\rho^\mu(p_3)\epsilon_\rho^\nu(p_4), \tag{B6}$$

$$\mathcal{M}^{(c)} = i\left(\frac{g}{\sqrt{2}}\right)^2 \left\{\left[1 + 4\frac{c_1}{f_\pi^2}p_3\cdot p_4 - \frac{c_2}{f_\pi^2}(p_1 + p_2)^2\right]g_{\mu\nu} - 4\frac{c_1}{f_\pi^2}p_{4\mu}p_{3\nu} + 2\frac{c_2}{f_\pi^2}p_{4\mu}p_{3\nu}\right\}\epsilon_\rho^\mu(p_3)\epsilon_\rho^\nu(p_4). \tag{B7}$$

The invariant scattering matrix element is given by

$$\mathcal{M}(\pi^+ + \pi^- \to \rho^0 + \rho^0) = \mathcal{M}(\pi^0 + \pi^0 \to \rho^+ + \rho^-) = \mathcal{M}^{(a)} + \mathcal{M}^{(b)} + \mathcal{M}^{(c)}. \tag{B8}$$

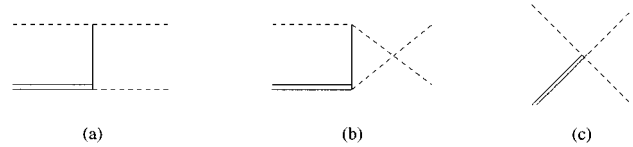

FIG. 11. Same as Fig. 10 for the reactions $\pi^+ + a_1^- \to \pi^0 + \pi^0$ and $\pi^+ + a_1^+ \to \pi^+ + \pi^+$.

2. $\pi + \pi \to \pi + \omega$

The related diagrams are shown in Fig. 9. The explicit expression for the invariant matrix element is

$$\mathcal{M}(\pi + \pi \to \pi + \omega) = \mathcal{M}^{(a)} + \mathcal{M}^{(b)} + \mathcal{M}^{(c)}, \tag{B9}$$

where

$$\mathcal{M}^{(a)} = ig_{\omega\rho\pi}\frac{g}{\sqrt{2}}\left(1 - \frac{\delta}{2m_\rho^2}(p_1 - p_3)^2\right) \times \epsilon^{\mu\nu\alpha\beta}\frac{(p_{1\alpha} + p_{3\alpha})(p_{1\beta} - p_{3\beta})}{(p_1 - p_3)^2 - m_\rho^2}\epsilon_\mu^\omega(p_4)p_{4\nu}, \tag{B10}$$

$$\mathcal{M}^{(b)} = ig_{\omega\rho\pi}\frac{g}{\sqrt{2}}\left(1 - \frac{\delta}{2m_\rho^2}(p_3 - p_2)^2\right) \times \epsilon^{\mu\nu\alpha\beta}\frac{(p_{3\alpha} + p_{2\alpha})(p_{1\beta} - p_{4\beta})}{(p_1 - p_4)^2 - m_\rho^2}\epsilon_\mu^\omega(p_4)p_{4\nu}, \tag{B11}$$

$$\mathcal{M}^{(c)} = -ig_{\omega\rho\pi}\frac{g}{\sqrt{2}}\left(1 - \frac{\delta}{2m_\rho^2}(p_1 + p_2)^2\right) \times \epsilon^{\mu\nu\alpha\beta}\frac{(p_{1\alpha} - p_{2\alpha})(p_{1\beta} + p_{2\beta})}{(p_1 + p_2)^2 - m_\rho^2}\epsilon_\mu^\omega(p_4)p_{4\nu}. \tag{B12}$$

3. $\pi + a_1 \to \pi + \pi$

a. $\pi^+ + a_1^0 \to \pi^0 + \pi^+$, $\pi^+ + a_1^- \to \pi^+ + \pi^-$

The related diagrams are shown in Fig. 10. The explicit expression for the invariant matrix element for each reaction is given by

$$\mathcal{M}^{(a)} = -\left(\frac{g}{\sqrt{2}}\right)^2 \frac{1}{f_\pi}\frac{1}{(p_1 - p_3)^2 - m_\rho^2}\left(1 - \frac{\delta}{2m_\rho^2}(p_1 - p_3)^2\right)\{[\eta_1 p_4\cdot(p_1 - p_3) - \eta_2 p_2\cdot(p_1 - p_3)](p_{1\mu} + p_{3\mu}) - [\eta_1 p_4\cdot(p_1 + p_3) - \eta_2 p_2\cdot(p_1 + p_3)](p_{1\mu} - p_{3\mu})\}\epsilon_{a_1}^\mu(p_2), \tag{B13}$$

$$\mathcal{M}^{(b)} = -\left(\frac{g}{\sqrt{2}}\right)^2 \frac{1}{f_\pi}\frac{1}{(p_1 + p_2)^2 - m_\rho^2}\left(1 - \frac{\delta}{2m_\rho^2}(p_1 + p_2)^2\right)\{[\eta_1 p_1\cdot(p_1 + p_2) + \eta_2 p_2\cdot(p_1 + p_2)](p_{3\mu} - p_{4\mu}) - [\eta_1 p_1\cdot(p_3 - p_4) + \eta_2 p_2\cdot(p_3 - p_4)](p_{3\mu} + p_{4\mu})\}\epsilon_{a_1}^\mu(p_2), \tag{B14}$$

$$\mathcal{M}^{(c)}=\frac{1}{f_\pi^3}\{(2d_1f_\pi^2+2d_2p_3\cdot p_4-2d_3p_2\cdot p_3)p_1^\mu-(2d_1f_\pi^2-2d_2p_1\cdot p_3-2d_3p_2\cdot p_3)p_4^\mu$$
$$+[4d_1f_\pi^2-4d_2p_1\cdot p_4+2d_3(p_1-p_4)\cdot p_2]p_3^\mu\}\epsilon_{a_1}^\mu(p_2), \tag{B15}$$

where d_i's are given by parameters in the Lagrangian. See Appendix A.

The invariant matrix element is given by

$$\mathcal{M}(\pi^+ + a_1^0\to\pi^0+\pi^+)=\mathcal{M}(\pi^+ + a_1^-\to\pi^+ + \pi^-)=\mathcal{M}^{(a)}+\mathcal{M}^{(b)}+\mathcal{M}^{(c)}. \tag{B16}$$

b. $\pi^+ + a_1^- \to \pi^0 + \pi^0$, $\pi^+ + a_1^+ \to \pi^+ + \pi^+$

The related diagrams are shown in Fig. 11. The explicit expression for the invariant matrix element for each reaction is given by

$$\mathcal{M}^{(a)}=-\left(\frac{g}{\sqrt{2}}\right)^2\frac{1}{f_\pi}\frac{1}{(p_1-p_3)^2-m_\rho^2}\left(1-\frac{\delta}{2m_\rho^2}(p_1-p_3)^2\right)\{[\eta_1p_4\cdot(p_1-p_3)-\eta_2p_2\cdot(p_1-p_3)](p_{1\mu}+p_{3\mu})$$
$$-[\eta_1p_4\cdot(p_1+p_3)-\eta_2p_2\cdot(p_1+p_3)](p_{1\mu}-p_{3\mu})\}\epsilon_{a_1}^\mu(p_2), \tag{B17}$$

$$\mathcal{M}^{(b)}=-\left(\frac{g}{\sqrt{2}}\right)^2\frac{1}{f_\pi}\frac{1}{(p_1-p_4)^2-m_\rho^2}\left(1-\frac{\delta}{2m_\rho^2}(p_1-p_4)^2\right)\{[\eta_1p_3\cdot(p_1-p_4)-\eta_2p_2\cdot(p_1-p_4)](p_{1\mu}+p_{4\mu})$$
$$-[\eta_1p_3\cdot(p_1+p_4)-\eta_2p_2\cdot(p_1+p_4)](p_{1\mu}-p_{4\mu})\}\epsilon_{a_1}^\mu(p_2), \tag{B18}$$

$$\mathcal{M}^{(c)}=\frac{1}{f_\pi^3}\{[4d_1f_\pi^2+4d_2p_3\cdot p_4-2d_3(p_4+p_3)\cdot p_2]p_1^\mu-(-2d_1f_\pi^2+2d_2p_1\cdot p_4-2d_3p_1\cdot p_2)p_3^\mu$$
$$-(-2d_1f_\pi^2+2d_2p_1\cdot p_3-2d_3p_1\cdot p_2)p_4^\mu\}\epsilon_{a_1}^\mu(p_2). \tag{B19}$$

The invariant scattering matrix element is given by

$$\mathcal{M}(\pi^+ + a_1^-\to\pi^0+\pi^0)=\mathcal{M}(\pi^+ + a_1^+\to\pi^+ + \pi^+)=\mathcal{M}^{(a)}+\mathcal{M}^{(b)}+\mathcal{M}^{(c)}. \tag{B20}$$

[1] For a recent review see Quark Matter '95 [Nucl. Phys. **A590**, 1 (1995)].
[2] E. V. Shuryak, Phys. Rep. **61**, 71 (1980); L. McLarren, Rev. Mod. Phys. **58**, 1001 (1986).
[3] E. Shuryak, Phys. Rev. Lett. **68**, 3270 (1992).
[4] T. Biró, E. Doorn, B. Müller, M. Thoma, and X. Wang, Phys. Rev. C **48**, 1275 (1993); X.-N. Wang, Nucl. Phys. **A590**, 47c (1995).
[5] K. Geiger and J. Kapusta, Phys. Rev. D **47**, 4905 (1993).
[6] J. Stachel and P. Braun-Munzinger, Phys. Lett. B **216**, 1 (1989).
[7] P. Braun-Munzinger, J. Stachel, J. Wessels, and N. Xu, Phys. Lett. B **344**, 43 (1995).
[8] P. Braun-Munzinger, J. Stachel, J. Wessels, and N. Xu, Phys. Lett. B **365**, 1 (1996).
[9] J. Rafelski, Phys. Lett. B **262**, 333 (1991); J. Letessier, A. Tounsi, and J. Rafelski, *ibid.* **292**, 417 (1992); J. Letessier, J. Rafelski, and A. Tounsi, *ibid.* **328**, 499 (1994).
[10] N. J. Davidson, H. G. Miller, R. M. Quick, and J. Cleymans, Phys. Lett. B **255**, 105 (1991).
[11] J. Sollfrank, M. Gaździcki, U. Heinz, and J. Rafelski, Z. Phys. C **61**, 659 (1994); U. Heinz, Nucl. Phys. **A566**, 205c (1994).
[12] J. Sollfrank and U. Heinz, in *Quark-Gluon Plasma 2*, edited by R. C. Hwa (World Scientific, Singapore, 1996).
[13] J. Gasser and H. Leutwyler, Phys. Lett. B **184**, 83 (1987); P. Gerber and H. Leutwyler, Nucl. Phys. **B321**, 387 (1989).
[14] J. L. Goity and H. Leutwyler, Phys. Lett. B **228**, 517 (1989); Chungsik Song, Phys. Rev. D **48**, 1556 (1994); K. Haglin and S. Pratt, Phys. Lett. B **328**, 255 (1994).
[15] K. Haglin, Nucl. Phys. **A584**, 719 (1995); C. Song and C. M. Ko, Phys. Rev. C **53**, 2371 (1996).
[16] T. Matsui, B. Svetitsky, and L. McLerran, Phys. Rev. D **34**, 783 (1986); **34**, 2047 (1986).
[17] J. L. Goity, Phys. Lett. B **319**, 401 (1993).
[18] D. Lohse, K. W. Durso, K. Holinde, and J. Speth, Phys. Lett. B **234**, 235 (1990).
[19] G. F. Bertsch and S. Das Gupta, Phys. Rep. **160**, 189 (1988).
[20] P. Danielewicz and G. F. Bertsch, Nucl. Phys. **A533**, 712 (1991).
[21] H. Bebie, P. Gerber, J. L. Goity, and H. Leutwyler, Nucl. Phys. **B378**, 95 (1992).
[22] U.-G. Meissner, Phys. Rep. **161**, 213 (1988).
[23] Chungsik Song, Phys. Rev. C **47**, 2861 (1993).
[24] E. Written, Nucl. Phys. **B223**, 432 (1983); Ö. Kaymakcalan, S. Rajeev, and J. Schechter, Phys. Rev. D **30**, 594 (1984).